Journal of Non-Crystalline Solids 528 (2020) 119713

Contents lists available at ScienceDirect

Journal of Non-Crystalline Solids

journal homepage: www.elsevier.com/locate/jnoncrysol

Hot-pressing of Tellurite glass with a sacrificial pressure-transmitting medium

Daniel McGill[a,b,*], Justine Ben Ghozi-Bouvrande[a,b,c], Myungkoo Kang[a], Morgane Dolhen[c], Gaëlle Delaizir[c], Sebastien Chenu[c], Léna Roumiguier[a,b,c], Jean-René Duclère[c], Kathleen A. Richardson[b], Romain Gaume[a]

[a] Optical Ceramics Laboratory, University of Central Florida, Orlando, FL 32816, United States
[b] Glass Processing and Characterization Laboratory, University of Central Florida, Orlando, FL 32816, United States
[c] Institut de Recherche sur les Céramiques (IRCER), UMR 7315 CNRS, Centre Européen de la Céramique, Limoges, France

ARTICLE INFO

Keywords:
Glass powder densification
Sintering
Infrared glass

ABSTRACT

Glass powder of composition $70TeO_2$-$20WO_3$-$10La_2O_3$ (mol%) was sintered to high density within a hot-press using a sacrificial powder as a pressure-transmitting medium. The potassium chloride (KCl) sacrificial power was found to minimize sample friction and adhesion to the die during pressing, facilitated the extraction of the densified sample from the die and was easily removable due to its water solubility. This fabrication process maximizes pressure transference to the green-body and enables sintered parts with optical quality comparable to those obtained by the melt-quench technique.

1. Introduction

Solid-state pressure-transmitting medium can be used to form complex-shaped samples by hot-pressing, without the use of convoluted die configurations [1–5]. This pressure-transmitting medium can be chosen to facilitate demolding. When introduced in the powder form, this pressure-transmitting medium maintains high flowability during the initial stage of sintering and provides an isostatic state-of-stress around the green-body. As densification proceeds, this condition can evolve towards a non-uniform state-of-stress due to a decrease in the transmitted pressure near the die walls, and yield concave-shaped sintered bodies [5]. However, the magnitude of this deviatoric stress can be reduced by using a highly plastic pressure-transmitting powder [1] or by adjusting the die aspect and filling ratios. This fabrication method can be applied to the sintering of glasses, glass-ceramics and in the manufacture of glass composites. In addition, the pressure-transmitting phase can also serve as a diffusion-barrier to prevent contamination from the die and, for example, limit oxidation–reduction reactions between a graphite die and an oxide sample.

To illustrate the potential of this technique, we investigated the sintering of tellurite $70TeO_2$-$20WO_3$-$10La_2O_3$ (TWL) (mol%) glass powders using potassium chloride (KCl) as the sacrificial pressure-transmitting medium. Tellurium dioxide based glasses are highly soluble to rare-earth elements which makes them well suited as laser sources, amplifiers and optical fibers [6–9]. TWL glasses have also been shown to be highly stable to crystallization [10,11] which makes it an ideal candidate for sintering . KCl was selected as the candidate of choice due to its face-centered cubic structure and the many active slip systems this crystalline structure provides. Compared to other isostructural salts, the high plasticity of KCl was found to be well-suited at transferring applied pressure to the TWL glass powders.

2. Material and methods

Powders used in the effort were prepared from parent glasses made by traditional melt/quench methods. The parent TWL glass was prepared from the following constituent oxides: 99.9% TeO_2 from Todini, 99.8% WO_3 from Alfa Aesar and 99.99% La_2O_3 from Rhône-Poulenc. These oxides were placed in a high purity platinum crucible where they were melted at 850 °C for one hour in air and stirred four times to remove trapped air bubbles and homogenize the melt constituents. Melting times for tellurite glasses are typically short, as melt volatilization can occur during extended melt times changing the composition of the melt. The homogenized melt was then quenched between two room temperature brass plates. The as-quenched 'parent' bulk glass was ground into powders, sieved, and classified by grain size in batches of coarse (100 to 250 μm) and fine (smaller than 100 μm) powders. A microscope image of the TWL parent-bulk glass is shown in Fig. 1. A

* Corresponding author at: Optical Ceramics Laboratory, University of Central Florida, Orlando, FL 32816, United States
E-mail address: danieljmcgill@knights.ucf.edu (D. McGill).

https://doi.org/10.1016/j.jnoncrysol.2019.119713
Received 4 July 2019; Received in revised form 17 September 2019; Accepted 23 September 2019
Available online 12 November 2019

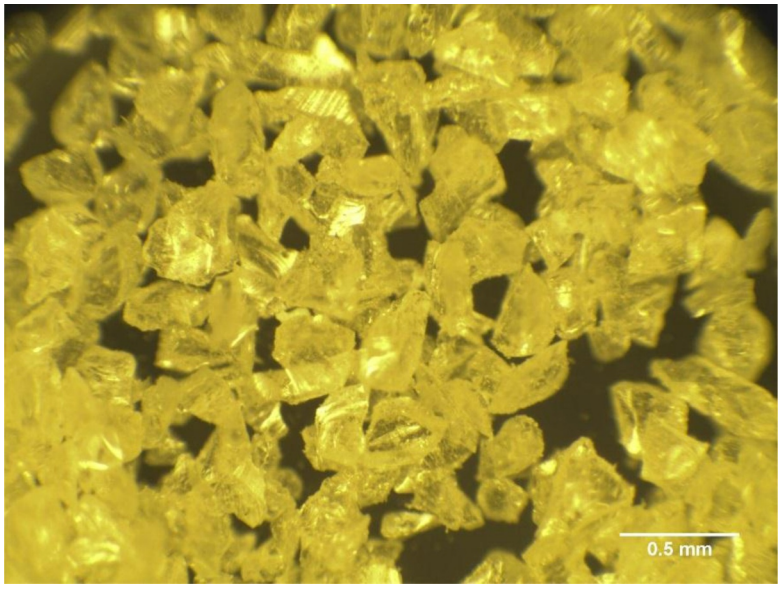

Fig. 1. Optical micrograph of $70TeO_2$-$20WO_3$-$10La_2O_3$ (TWL) coarse glass powder. Particle size ranges from 100 to 250 μm.

sample of the bulk parent glass (post-annealed) was used for comparisons of density, index of refraction and transmission. As hydroxyl groups are a common impurity in TWL glass compositions [12], leading to infrared absorption loss [6], batch raw materials, post-processed parent glass and post-sized powders need to be stored in desiccators to minimize adsorbed moisture.

3. Experimental

Differential scanning calorimetry (DSC) was used to determine the glass transition temperature and first crystallization peak of the parent glass powders and from this information a target sintering temperature was selected. This target temperature was chosen to avoid crystallization and yet be of high enough temperature to achieve rapid densification.

Glass sintering experiments were carried out by cold-pressing 20 g of coarse TWL glass powder under rough vacuum ($> 10^{-3}$ torr) within a uniaxial steel die to form the initial green-body. 'Coarse' powder was chosen for the sintering process as it was previously found that 'fine' particles poorly densified. The resulting green-body was surrounded by KCl powder, which had previously been stored within a 100 °C oven until use. The encapsulated preform was loaded into a separate steel die placed in an airtight hot-press container [13]. This container, shown in Fig. 2, allows for flushing of inert gas and drawing of rough vacuum while being able to compress under a uniaxial load. Multiple vacuum-compatible feedthroughs exist on the device for electrical connections and thermocouples. A resistive coil heater and PID controller were used for temperature control.

A thermocouple was inserted into the body of the sleeve near the sample location and the die was sealed within the vessel. The container was brought to rough vacuum and then flushed with argon gas three times and then held at rough vacuum for the remainder of the sintering experiment. The vessel was heated and held at the soak temperature, which was selected to be above the glass transition but far below crystallization, while being pressed down upon by a die press for a period of approximately 15 min. Then the pressure was released, and the die was cooled. The TWL, encapsulated in KCl, was extracted from the die and placed in water to dissolve the KCl. The sintered glass sample was then polished before transmission and index of refraction measurements.

The density of the resulting sintered glass specimen and the parent bulk melt/quench glass were determined by the Archimedes' method

Fig. 2. Vacuum-compatible compressible container used in the sintering experiments. Feedthroughs for a vacuum and gas line along with thermocouple are shown connected to the base. A die press is shown pressing on the vessel which in turn applies pressure on a steel die located inside.

using an Adam Equipment PW 254 analytical balance with an added density kit. The samples were suspended in deionized water at 21 °C and the density is the average of five measurements with error calculated from the standard deviation of these measurements. Differential scanning calorimetry (DSC) measurements were performed on sample powders of approximately 20 mg mass using a DSC204 F1 Phoenix device with aluminum pans at a heating rate of 5 °C/min. The glass transition temperature was calculated by finding the peak of the first derivative of the heat flow signal and the onset of crystallization via the intercept method and the error was estimated to be ± 2 °C. These

measurements were used to compare crystallization behavior as an indicator of possible ceramization. X-ray diffraction (XRD) analyses were carried on bulk and sintered glass samples using a Malvern PANalytical Empryrean device with a copper X-ray tube. The raw data was processed using Highscore software where background was removed, and the diffraction peaks due to the presence of the $K_{\alpha 2}$ line of Cu stripped from the data. Electron dispersive X-ray spectroscopy (EDS) was used to determine if potassium or chlorine were present within the sintered samples, either on the surface or in the bulk. EDS measurements were performed using a Zeiss ULTRA-55 FEG scanning electron microscope (SEM) equipped with Noran System 7 EDS. A reference spectrum was collected by taking the average of five normalized spectra obtained from the top of a polished melt/quench sample. This reference spectrum was subtracted from an average of eleven spectra obtained from the top surface of the sintered sample (closest to the steel top plunger). The limited thickness of the sintered sample made the contribution from the conductive silver paste and aluminum sample holder unavoidable.

The optical quality of the sintered samples was evaluated by comparing their transmission spectrum and index of refraction to that of a melt/quench bulk glass of same composition. The index of refraction was measured at multiple wavelengths using a Metricon 2010 M system modified for use in the infrared as described in [14]. The index of refraction measured at five wavelengths was fitted using a Sellmeier equation. The transmission measurements were performed using a Thermo Scientific Nicolet iS5 Fourier transform infrared spectrometer.

4. Results

To interpret the results of the TWL glass sintering process and role of the sacrificial KCl powder on the resulting post-sintered material's physical properties, the characteristics of the parent, bulk, TWL glass was compared to that of the post-sintered glass sample (TWL sample 20).

4.1. Sintered sample physical appearance

Extraction of intact samples from the die following pressing was a challenge throughout the study. However, improvements that led to parts over a centimeter in size were realized with the use of KCl powder where samples could be more readily demolded from the die without fracture. Prior to its use, glass samples would adhere to the body of the steel die or flow between the die parts causing die seizing. With KCl, the part could be extracted intact, with limited fractures in its bulk resulting from either thermal and/or mechanical stresses arising through the press schedule (Fig. 3a).

Once the sample was extracted from the die, the KCl encapsulant surrounding the sintered TWL part was removed by dissolving it in water. While the KCl could be completely dissolved with this process, some artifacts from the powder were seen on the as-pressed part prior to polishing. Surfaces of the TWL sintered samples were found to exhibit a roughened surface with texture due to the 'imprint' pattern from deformed and densified KCl in intimate contact with the sintered part during pressing as shown in (Fig. 3b/c). Upon polishing this roughness was removed. All as-pressed samples exhibited a slight haziness and dispersed dark brown inclusions (Fig. 3a) which is evident when compared to a melt/quench TWL bulk glass (Fig. 3d). The dark brown spots scattered in the majority of the sintered samples are similar to those seen in SPS samples induced by carbon contamination [15]. Nevertheless, our efforts to determine the origin of these spots have not yet been conclusive as many efforts were made to reduce carbon contamination from trapped CO_2 and CO gases within the process without noticeable impact on the occurrence of the inclusions. Therefore, the possibility that these dark brown inclusions may also be color-centers or localized tungsten reduction has not been ruled out.

4.2. Thermal, microstructural and optical properties of sintered twl glass

The density of the TWL sintered sample glass was measured and found to be 6.09 ± 0.01 g/cm^3 compared to that of the parent TWL bulk glass of 6.07 ± 0.02 g/ cm^3. Full densification was achieved but the difference in thermal history between bulk and sintered specimens, makes a direct comparison difficult. The density of the sintered glass slightly exceeds that of the unannealed starting powder from which the part derives. The density of the TWL bulk glass and TWL sintered sample glass are within the margin of error of the measurement technique and thus any difference between them, is likely attributable to this difference in thermal history from the anneal and sintering processes. The results indicate that well-densified samples can be obtained through a sacrificial powder approach using KCl.

To determine whether the sintering process has modified the extent of crystallization in the post-processed part, DSC was carried out on the sintered sample and compared to the starting (coarse) powder, as shown in Fig. 4. As can be seen, the sintered sample has a fully resolved crystallization peak near 510 °C which has been shown to be associated with surface forming $La_2Te_6O_{15}$ crystalline phase in research with same composition glasses by Dohlen [16]. Fujimoto et al. also observed this crystalline phase in a similar composition tellurite glass [17]. This larger exotherm in the sintered samples is likely due to traces of the original grain boundaries. However, it may also be the case that some additional level of crystallization occurred during the reheating of the glass powder in the sintering process. The temperatures associated with the various DSC results for each sample, has been compiled in Table 1.

In order to further assess whether crystallization has occurred during sintering, XRD was performed on the TWL sintered glass and the parent coarse glass powder. Specimens were both ground and sieved to select for particle size smaller than 75 μm in order to avoid size-dependent differences in XRD results. The results of this powder diffraction measurement are shown in Fig. 5 where blue drop lines have been added to denote the crystalline $La_2Te_6O_{15}$ phase. As noted above, this crystal phase, while not readily apparent in the parent or sintered part, is believed to be associated with the lower temperature crystallization peak observed in DSC near 510 °C. It appears that either crystallization did not occur, or it is below the level of detection of XRD owing to being too small in size and volume fraction.

EDS shows that potassium and chlorine from the sacrificial powder

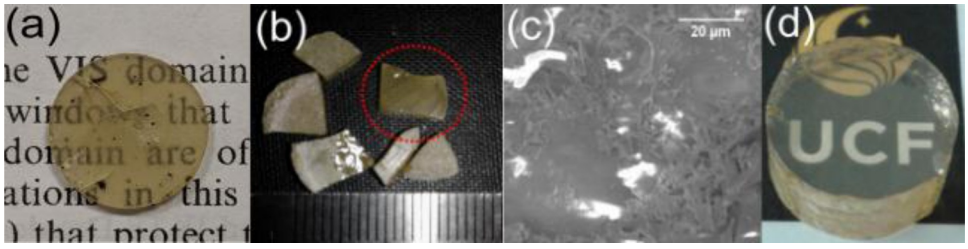

Fig. 3. (a) Example of a sintered TWL glass pellet obtained by hot-pressing with KCl sacrificial powder. The sample is shown after polishing and is 1 mm thick. (b) Sintered TWL fragments illustrating the surface roughness of the unpolished glass. The upper right piece pictured here (circled) has been partially polished to show the difference in surface texture. (c) SEM image of the rough surface before polishing. (d) the bulk melt/quenched TWL parent glass showing the difference in coloration when compared to (a). (For interpretation of the references to colour in this figure legend, the reader is referred to the web version of this article.)

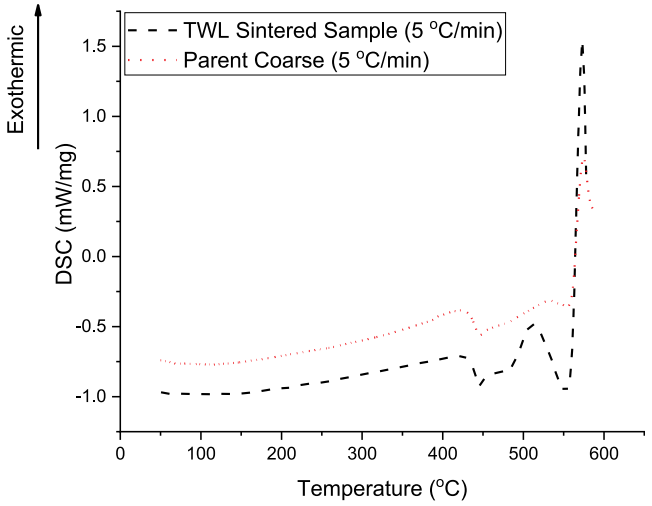

Fig. 4. DSC of TWL parent coarse powders and post-sintered TWL sample powder measured at heating rates of 5 °C/min.

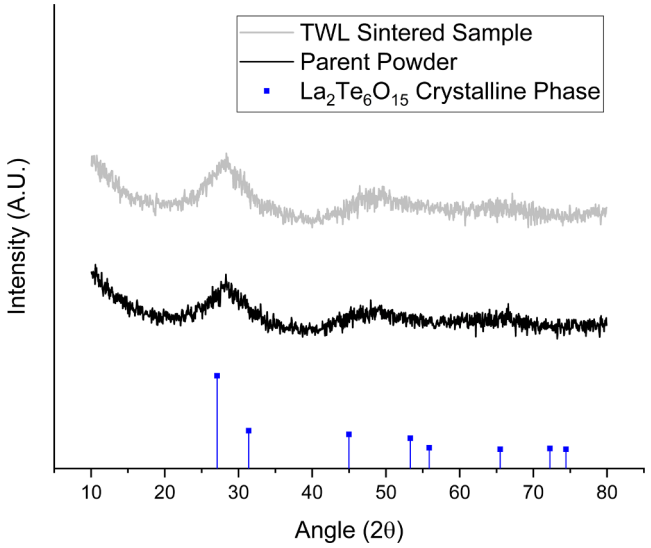

Fig. 5. Powder X-ray diffraction on sintered and parent TWL glasses with particle sizes < 75 μm. Drop lines have been added to show the pattern of $La_2Te_6O_{15}$ crystalline phase based upon JCPDS 00–043–0551.

do not appear to be present within the sintered sample. In Fig. 6, the regions where the potassium and chlorine peaks would be, if present, have been highlighted and no detectable contribution from either is seen. Therefore, contamination from the sacrificial powder can be ruled out as a contributing factor for both the increased density and any changes to the index of refraction or absorption spectrum.

The index of refraction of both the bulk glass and sintered TWL sample were obtained at multiple wavelengths within the glass' mid-wave infrared transmission region and fitted with a Sellmeier equation as shown in Fig. 7a. The coefficients obtained for the Sellmeier equation for these two fits are provided in Eq. (1).

$$\text{Bulk: } n^2 = 4.59035 + \left(\frac{2.59245^2 * \lambda^2}{\lambda^2 - 19.8026^2}\right)$$
$$\text{TWL Sintered Sample: } n^2 = 4.5421 + \left(\frac{2.78466^2 * \lambda^2}{\lambda^2 - 21.10078^2}\right) \quad (1)$$

Eq. (1). Sellmeier equations for TWL bulk and sintered glasses.

As illustrated in Fig. 7a there is a measurable change in refractive index realized upon sintering as compared to the parent bulk TWL glass. This difference is 0.71% at 4 μm. This difference cannot be due to nanocrystallization since the increased density of the crystalline phase would cause an increase in refractive index which is not observed here. Change in composition is also unlikely due to the sintering temperature being well below the melt temperature and the observation that loss-on-ignition (due to TeO_2 departure) being negligible below the melting point of tellurites [18]. Hence, with the previous evidence of negligible density change and lack of observed crystalline phase formation via XRD, it is inferred that the very minor index variation is due to either a difference in thermal history, residual porosity or both.

Fig. 7b illustrates the infrared transmission variation of the parent bulk glass to that of the sintered TWL material. Samples were measured at the same time, taking care to ensure that the sample chamber was dry and purged with N_2. The sintered TWL has a greater loss in the near-IR than that of same parent glass composition indicating that absorption and scatter may be higher in the sintered part. No UV–VIS spectrophotometry was made on these samples. These data indicate moisture contribution to the processed part, and the possibility of scattering

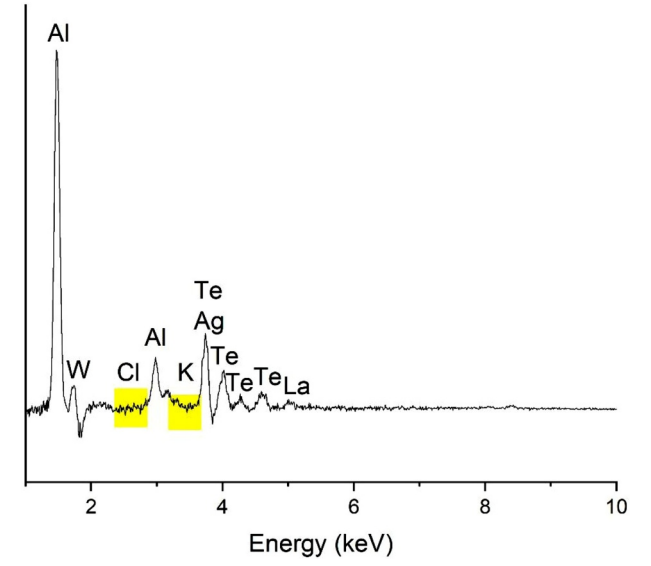

Fig. 6. EDS spectra acquired from the top surface of a sintered TWL sample with the melt/quench spectra subtracted. The regions where Cl and K contamination would appear, if present, have been highlighted. The Al and Ag peaks are experimental artifacts from the sample holder and conductive paste, respectively.

centers from microcrystals or residual porosity. Hence, atmospheric moisture and CO_2 were minimized. Despite these efforts a new absorption band near 4.3 μm is observed in the sintered part, suggesting that even with multiple flushing cycles with Ar during the vacuum sintering process, some atmospheric contamination to the sintered part may be occurring. This feature has been well documented in other tellurite compositions where atmospheric moisture content in the bulk material, can be eliminated in doped glasses where re-absorption of

Table 1
Tabulated results of the DSC measurements shown in Fig. 4. Temperature values are given within ± 2 °C.

Sample Type	Heating Rate (°C/min)	Mass (mg)	T_g (°C)	T_{p1} (°C)	T_{p2} (°C)
TWL Sintered Sample	5	20.7	442	510	573
Parent-Coarse	5	24.7	441	Unresolved	575

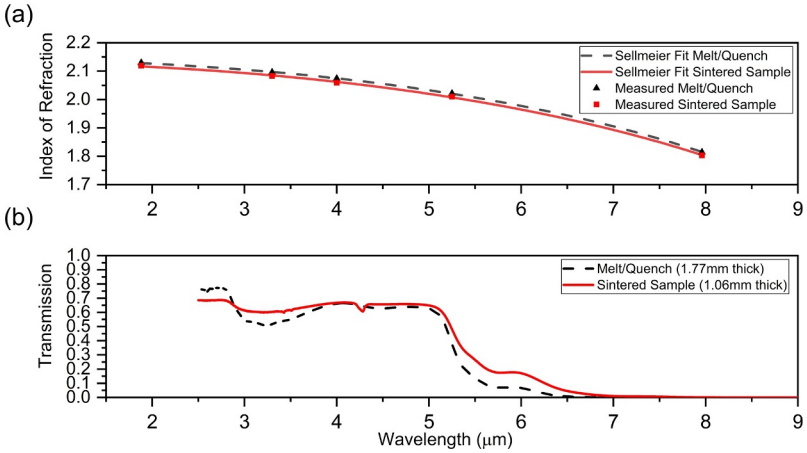

Fig. 7. (a) Index of refraction measurements obtained through use of a prism coupler method. These measurements are fitted with a Sellmeier equation. Errors in the refractive index measurements are less than 0.0006 (b) Transmission spectra of sintered and parent bulk glasses.

luminescence is problematic [19]. No significant change in the long-wave (multiphonon) absorption edge was noted suggesting that the processing protocol used to realize the sintered glass part, does not adversely impact the spectral window beyond those issues noted.

5. Conclusion

TWL glass powders can be densified to high density using potassium chloride as an encapsulant within a uniaxial hot-press. The high plasticity and water solubility of KCl simplifies the demolding of the glass sample from the die and simplifies the removal of the salt from the glass after processing. The low melting temperature of KCl precludes its use with the sintering of many glasses but is well suited to the sintering of many IR transparent optical glasses and glass ceramics. A TWL glass sample sintered via this process may have a small amount of nuclei as indicated by thermal analysis, though not clearly evident via XRD. The experimental process adopted prevents the contamination of the TWL sintered samples by the KCl sacrificial powder. This sintering process has a measurable impact on the index of refraction when compared to glass processed by a traditional melt/quench process due to differences in thermal history and the possible presence of residual porosity. Further process optimization on this glass is necessary to further reduce optical loss.

This method of using KCl, or other highly plastic salts with similar or higher melting points, as a sacrificial powder may be valuable in SPS in creating complex shapes and the co-sintering of glass and crystalline powders to create near net shape glass-ceramics or in the reduction of carbon contamination in SPS.

Funding

This research did not receive any specific grant from funding agencies in the public, commercial, or not-for-profit sectors.

Declaration of Competing Interest

The authors declare that they have no known competing financial interests or personal relationships that could have appeared to influence the work reported in this paper.

Acknowledgments

We wish to thank the many researchers and staff at the University of Central Florida who assisted with this work including Cesar Blanco, Matthew Julian, Anupama Yadav, Claudia Gonçalves, and Kirk Scammon.

References

[1] G.D. BarbarasU.S.P. Office, Isostatic Hot Pressing of Refractory Bodies, The United States of America, 1969 (Ed.).
[2] J.B. BrennanU.S.P. Office, Manufacture of Precision Articles from Powdered Material, United States of America, 1950 (Ed.).
[3] J.M. Googin, L.M. McLaughlinU.S.P. Office, Method of Fabricating Articles from Powders, United States of America, 1966 (Ed.).
[4] J.M. Lepp, J.A. SlyhU.S.P. Office, Process of Making Refractory Bodies, United States of America, 1951 (Ed.).
[5] F. Lange, G. Terwilliger, Powder vehicle hot-pressing technique, Am. Ceramic Soc. Bull. 52 (1973) 563–565.
[6] M. Churbanov, G. Snopatin, E. Zorin, S. Smetanin, E. Dianov, V. Plotnichenko, V. Koltashev, E. Kryukova, I. Grishin, G. Butsin, Glasses of TeO_2-WO_3 and TeO_2-Wo_3-La_2O_3 systems for fiber optics, J. Optoelectron. Adv. Mater. 7 (2005) 1765–1772.
[7] X. Feng, C. Qi, F. Lin, H. Hu, Tungsten–tellurite glass: a new candidate medium for Yb^{3+}-doping, J. Non Cryst. Solids 256 (1999) 372–377.
[8] V. Dorofeev, A. Moiseev, M. Churbanov, G. Snopatin, A. Chilyasov, I. Kraev, A. Lobanov, T. Kotereva, L. Ketkova, A. Pushkin, High-purity teo–wo–(La_2O_3, Bi_2O_3) glasses for fiber-optics, Opt. Mater. (Amst) 33 (2011) 1911–1915.
[9] K. Li, G. Wang, J. Zhang, L. Hu, Broadband~ 2μm emission in Tm^{3+}/Ho^{3+} co-doped TeO_2–WO_3–La_2O_3 glass, Solid State Commun. 150 (2010) 1915–1918.
[10] L. Zhu, T. Xu, Q. Nie, X. Shen, Spectral properties and thermal stability of erbium-doped TeO_2-WO_3-La_2O_3 glass, J. Inorganic Mater. 21 (2006) 351–356.
[11] V. Dorofeev, A. Moiseev, M. Churbanov, T. Kotereva, A. Chilyasov, I. Kraev, V. Pimenov, L. Ketkova, E. Dianov, V. Plotnichenko, Production and properties of high purity TeO_2− WO_3−(La_2O_3, Bi_2O_3) and TeO_2− ZnO− Na_2O− Bi_2O_3 glasses, J. Non Cryst. Solids 357 (2011) 2366–2370.
[12] G. Guery, T. Cardinal, A. Fargues, V. Rodriguez, M. Dussauze, D. Cavagnat, P. Thomas, J. Cornette, P. Wachtel, J.D. Musgraves, K. Richardson, Influence of hydroxyl group on IR transparency of tellurite-based glasses, Int. J. Appl. Glass Sci. 5 (2014) 178–184.
[13] T.W. Shoulder, R. Locke, R.M. Gaume, Elastic airtight container for the compaction of air-sensitive materials, Rev. Sci. Instrum. 87 (2016) 063908.
[14] B. Gleason, Designing optical properties in infrared glass, in: S.C. Clemson, S.C. Clemson (Eds.), Materials Science and Engineering, 2015, p. 213.
[15] A. Bertrand, J. Carreaud, G. Delaizir, J.R. Duclère, M. Colas, J. Cornette, M. Vandenhende, V. Couderc, P. Thomas, A comprehensive study of the carbon contamination in tellurite glasses and glass-ceramics sintered by spark plasma sintering (SPS), J. Am. Ceramic Soc. 97 (2014) 163–172.
[16] M. Dohlen, Verres, vitrocéramiques et céramiques transparentes à base d'oxyde de tellure pour l'optique, Matériaux Céramiques, l'Université de Limoges, Limoges, France, 2018.
[17] Y. Fujimoto, Y. Benino, T. Fujiwara, R. Sato, T. Komatsu, Transparent surface and bulk crystallized glasses with lanthanide tellurite nanocrystals, J. Ceramic Soc. Japan 109 (2001) 466–469.
[18] J. Massera, Nucleation and growth behavior of tellurite-based glasses suitable for mid-infrared applications, Material Science and Engineering, Clemson University, Clemson, SC, 2009, p. 233.
[19] B.D.O. Richards, T. Teddy-Fernandez, G. Jose, D. Binks, A. Jha, Mid-IR (3–4 μm) fluorescence and ASE studies in Dy3+ doped tellurite and germanate glasses and a fs laser inscribed waveguide, Laser Phys. Lett. 10 (2013) 085802.